

# A Comparison of Exfoliation Methods on Microstructure and Electrochemical Performance of Graphene Nanosheets for Supercapacitors

Xinlu Li\*, Hongfang Song, Hao Wang, Hongyi Li, Yuxin Zhang and Jiamu Huang

College of Materials Science and Engineering, Chongqing University, Chongqing, 400030, P. R. China

Received: October 27, 2011, Accepted: December 07, 2011, Available online: January 31, 2012

**Abstract:** Graphene nanosheets (GNS) were exfoliated by thermal expansion and microwave irradiation, respectively. The influence of exfoliation methods on GNS's surface structure and electrochemical property were analyzed. The porosity structure of GNS was measured by  $N_2$  adsorption. The  $N_2$  adsorption results proved that both the specific surface area and pore volume of the GNS exfoliated by thermal expansion are larger than those by microwave irradiation. And the surface morphology was observed by scanning electron microscopy and transmission electron microscopy. The electrochemical performance of the graphene nanosheets were comparatively tested by cyclic voltammetry and galvanostatic discharge-charge tests. The GNS via thermal expansion exhibited better electrochemical property with the specific capacity of 188 F/g at the current density of 0.1 A/g.

**Keywords:** graphene nanosheets, supercapacitor, thermal expansion, microwave irradiation

## 1. INTRODUCTION

Recently, supercapacitors have been extensively developed due to the increasing demand for both high energy density, power density and long durability [1]. The performance of supercapacitors is known to depend principally on electrode materials. The search for new electrode materials leads to high electrochemical properties and low cost. Graphene, as one-atom thick layer [2], attracts tremendous research interest for its potential applications [3-5]. In terms of high electronic conductivity, large specific surface area and rich chemistry, graphene has been recognized as one of the promising electrode materials for supercapacitors. To date, graphene can be prepared by various methods, such as mechanical cleavage of graphite [2], exfoliation of graphite oxide [6], solvothermal synthesis [7], chemical vapor deposition [8-10] and thermal decomposition [11-13]. Compared with other methods, exfoliation of graphite oxide would be the best promising way to prepare graphene for supercapacitors due to mass production at low cost. Among various exfoliation methods, thermal expansion [14] and microwave irradiation [15] have been widely used to synthesize graphene. It is known that the microstructure and the capacitance of the graphene depend a lot on the synthesis process. However, previous literatures never report on the effect of the two

exfoliation methods on the microstructure and electrochemical capacitance of graphene for supercapacitors.

In this paper, we will systemically compare the thermal expansion and microwave irradiation method on the microstructure and electrochemical performance of graphene for supercapacitors.

## 2. EXPERIMENTAL

All the chemicals were of analytical grade. Graphite oxide (GO) was prepared by an improved Hummers' method [16]. Firstly, 360 ml sulfuric acid (98 wt.%), 40 ml phosphoric acid (85 wt.%) and 5 g natural graphite (50 mesh) were mixed together in an ice water bath. 30 g  $KMnO_4$  was added slowly in portions at the reaction temperature below 20 °C. Then, the mixture was stirred continuously for 24 h. After adding water (400 ml),  $H_2O_2$  (30 ml), centrifugation and filtration, the GO was washed with de-ionized water until pH=7 and dried at 60 °C for 24h. Finally, some of the as-prepared GO was thermal expanded in a muffle oven at 500,800 and 1050 °C. In addition, some other GO was microwave-assistant expanded in a microwave oven at 500,700 and 800 W for about 20 s. The sample collected in the muffle oven was denoted as TEGN-500, TEGN-800 and TEGN-1050 while those in the microwave oven as MIGN-500, MIGN-700 and MIGN-800.

The morphology of GNS were observed by transmission electron microscopy (TEM, LIBRA 200FE) and field-emission scan-

\*To whom correspondence should be addressed: Email: lixinlu@cqu.edu.cn  
Phone: +86-23-65127940; Fax: +86-23-65127306

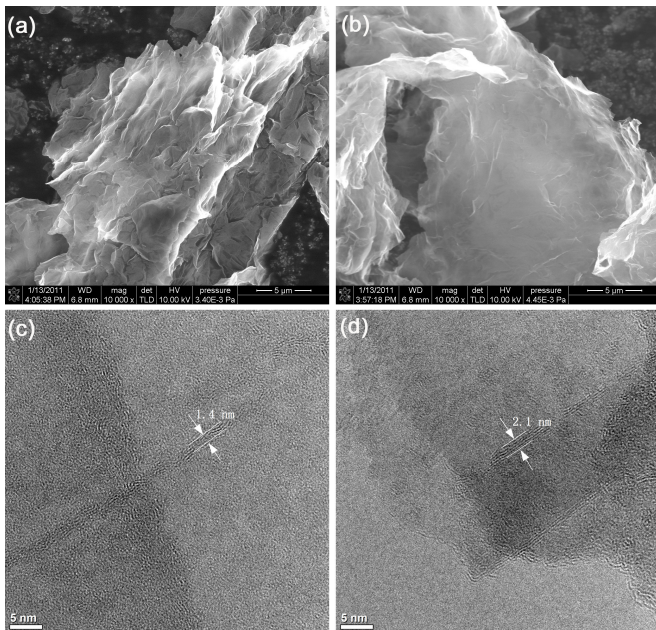


Figure 1. SEM images of (a) TEGN-1050 and (b) MIGN-800; HRTEM images of (c) TEGN-1050 and (d) MIGN-800.

ning electron microscopy (FESEM, ZEISS nova 400), respectively. Brunauer–Emmett–Teller (BET) specific surface area and pore size distribution were measured by nitrogen adsorption/de-adsorption using an automatic adsorption system (ASAP 2020 M).

The graphene electrode was prepared by loading the mixture of 80 wt.% of graphene, 10 wt.% carbon black and 10 wt.% of polyvinylidene difluoride on a nickel foam. All electrochemical measurements were done in a two electrode configuration. The measurements were conducted in a 6 M KOH aqueous electrolyte at room temperature. Cyclic voltammograms (CV) and galvanostatic charge/discharge were measured by Solartron (1260 8w). For the cyclic voltammetric measurements, the sweep rate ranged from 10, 25, 50, 100  $\text{mV s}^{-1}$  within the potential range of 0 to 1 V.

### 3. RESULTS AND DISCUSSION

Fig. 1 shows the morphology of TEGN-1050 and MIGN-800. From Fig. 1(a) and Fig. 1 (b), it can be seen that TEGN-1050 and MIGN-800 are both wrinkled and folded. The HRTEM image of TEGN-1050 in Fig. 1(c) indicates that TEGN-1050 is approximately 1.4 nm in thickness, composed of 4 wrinkled individual monoatomic graphene layers. And Fig. 1(d) suggests that the thickness of MIGN-800 is approximately 2.1 nm, which is made up of 6 wrinkled individual monoatomic graphene layers.

Table 1 is the data from the nitrogen adsorption measurement. The specific surface area of TEGN-1050 is  $469 \text{ m}^2/\text{g}$  while that of

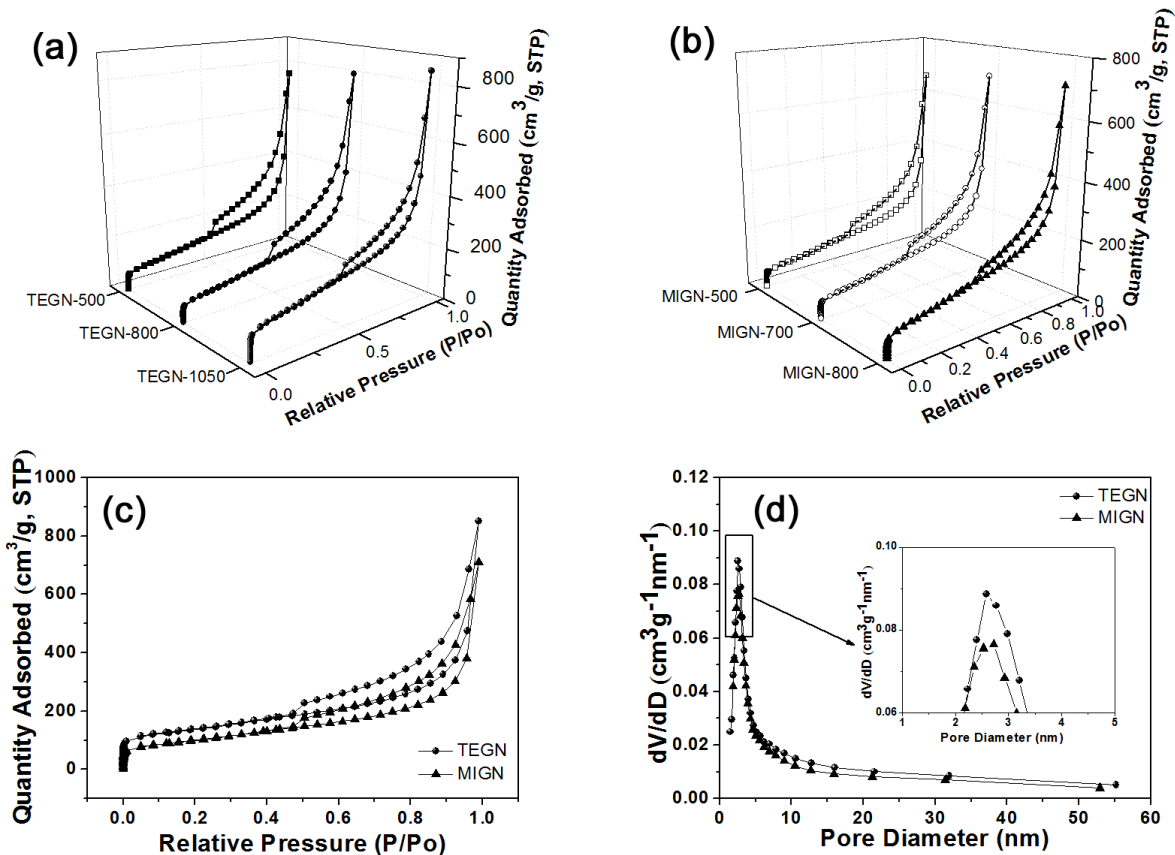


Figure 2. (a) Nitrogen adsorption/desorption isotherms of TEGN-500, TEGN-500, and TEGN-500; (b) Nitrogen adsorption/desorption isotherms of MIGN-500, MIGN-700, and MIGN-800 (c) Nitrogen adsorption/desorption isotherms of TEGN and MIGN; (d) The pore size distribution of TEGN and MIGN. The inset in (b) shows the enlarged image of the rectangle in (c).

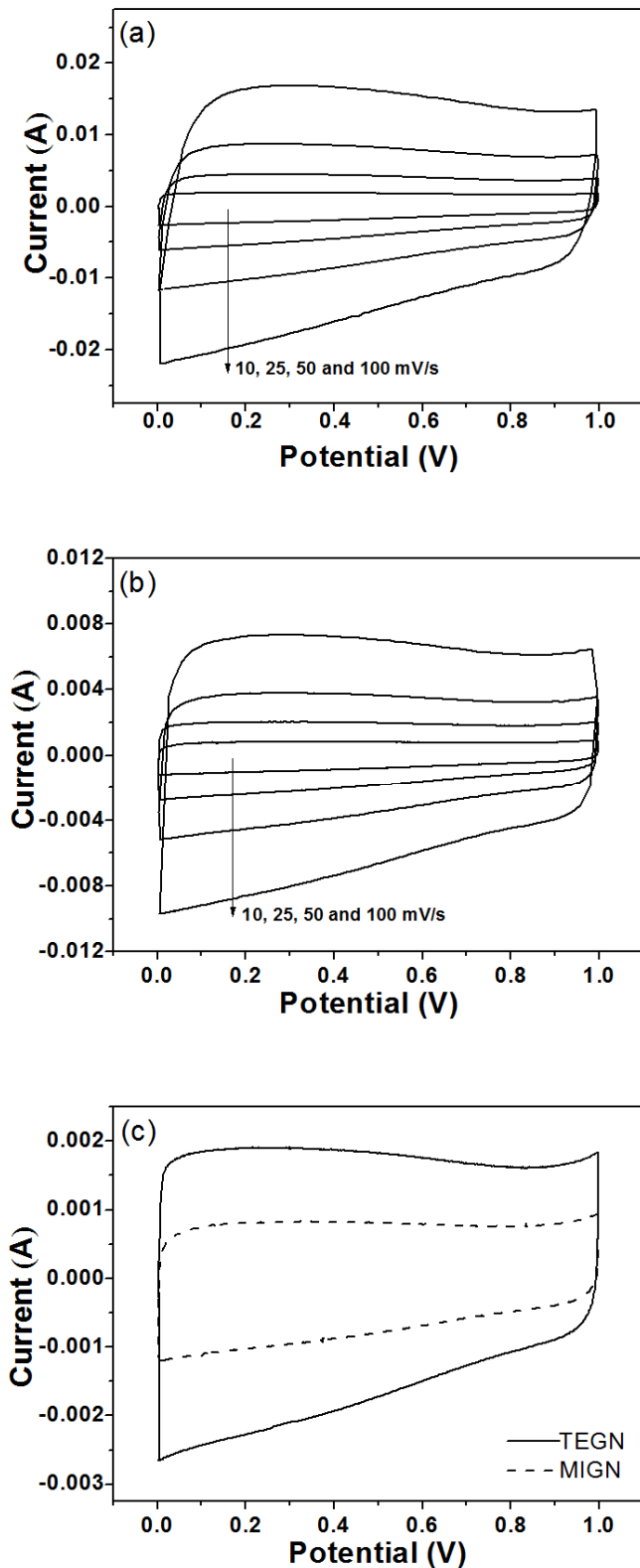


Figure 3. Cyclic voltammograms obtained from (a) TEGN electrode at different sweep rates, (b) MIGN electrode at different scan rates, (c) TEGN and MIGN electrodes at sweep rate of 10 mV/s.

MIGN-800 is 354 m<sup>2</sup>/g. Furthermore, the BET surface areas of TEGN-500 and TEGN-800 are about 317 m<sup>2</sup>/g and 325 m<sup>2</sup>/g, respectively while those of MIGN-500 and MIGN-700 are about 264 m<sup>2</sup>/g and 299 m<sup>2</sup>/g, respectively. It indicates that the GO is completely exfoliated neither for TEGN below 1050 °C nor MIGN below 800 W. Fig. 2a shows N<sub>2</sub> adsorption isotherms of TEGN-500, TEGN-800, and TEGN-1050. Obviously, all the three samples are characterized by type IV isotherms and possess hysteresis loops of type H3. The N<sub>2</sub> adsorption isotherms of MIGN-500, MIGN-700, and MIGN-800 in Fig. 2b can also be characterized by type IV isotherms. However, the N<sub>2</sub> quantity absorbed increases with temperature raising for TEGN or power raising for MIGN. The exfoliation of graphite oxide may occur below the temperature proposed by Schniepp et al.[14] or the power proposed by Zhu et al.[15], but the graphitic layers cannot be completely exfoliated. The electrochemical performance depends a lot on the specific surface area [17]. Therefore, TEGN-1000 (TEGN) and MIGN-800 (MIGN) are chosen to investigate the influence of exfoliation methods on microstructure and electrochemical performance of graphene nanosheets for supercapacitors.

Fig. 2(c) displays the nitrogen adsorption–desorption isotherms and Fig. 2(d) presents the pore size distribution curves calculated by Barrett–Joyner–Halenda (BJH) method. Fig. 2(c) showed that both TEGN and MIGN present the typical IV shapes according to IUPAC classification [18], indicating the mesoporous characteristics. As illustrated in Fig. 2(d), the pore size of TEGN and MIGN both mainly center around 2.5 nm. It is noted that the N<sub>2</sub> quantity absorbed by TEGN is higher than that by MIGN for all relative pressure (P/P<sub>0</sub>). According to the pore size distribution curves, the pore volume of TEGN is bigger than that of MIGN. The results prove that thermal expansion makes the graphene exfoliation more effectively, leading to the larger surface area and the bigger pore volume.

The thermal exfoliation method can cause the rapid expansion of CO or CO<sub>2</sub> gases from the interspace between graphene layers at instantaneous heating, resulting in the exfoliation of the graphite oxide [14]. In the case of microwave irradiation, the electrical spark can be generated from the inner space of graphite oxide and lead to exfoliation (Fig. 5). During the exfoliation for the former, the oxygen containing functional groups attached on parts of the basal planes near the edges are decomposed into gases and the gases go out of the interspace between the graphite oxide, leading to a great deal of mesopores. In the case of microwave irradiation, the exfoliation occurs at the inner in the graphite oxide where the electrical sparkles are generated. Consequently, MIGN leads to the lower pore volume and smaller surface area than TEGN.

The performance of the graphene-based electrodes is analyzed using CV and galvanostatic charge/discharge. The specific capacitance is calculated from the slope of the charge–discharge curves. The specific capacitance of the electrode is calculated according to the following equation [19]:

$$C_T = \frac{I \times \Delta t}{\Delta V} \quad (1)$$

$$\frac{1}{C_T} = \frac{1}{m_1 C_s} + \frac{1}{m_2 C_s} \quad (2)$$

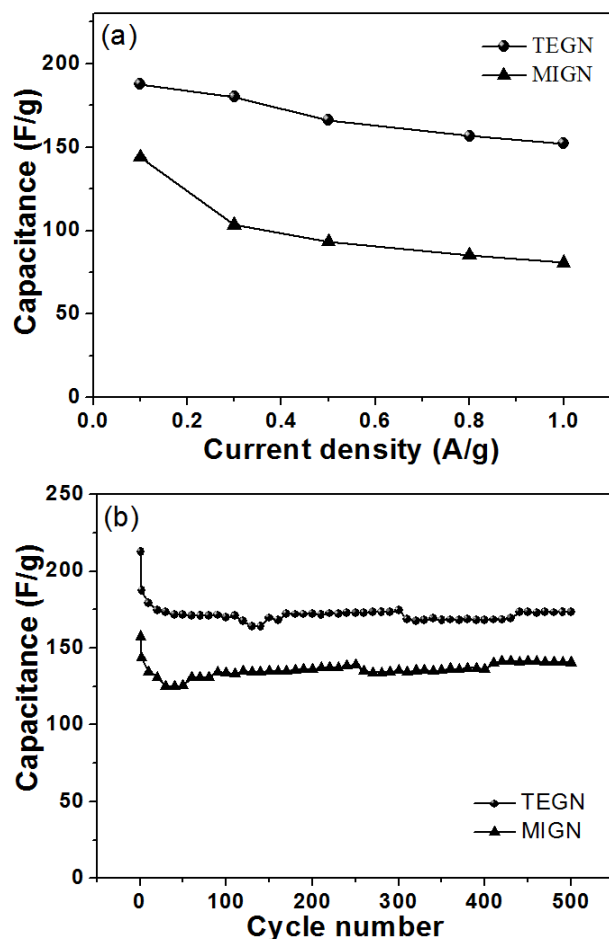


Figure 4. (a) Specific capacitance of TEGN and MIGN at different current density from 0.1 to 1.0 A/g in 6 M KOH solution; (b) Cycling performance of TEGN and MIGN under a current density of 0.1 A/g in 6 M KOH solution.

$C_T$  is the total series capacitance of the two electrodes in electrochemical capacitor cell (F),  $I$  is the current (A),  $\Delta t$  is the discharging time (s),  $\Delta V$  is the voltage difference of discharge (V),  $C_s$  is the specific capacitance of a single electrode (F/g),  $m_1$  and  $m_2$  are the active mass of the two electrodes, respectively.

Fig. 3 presents the CV curves of TEGN and MIGN in 6 M KOH aqueous electrolyte in the range of 0 to 1 V, respectively. In Fig. 3(a) and (b), both the two cyclic voltammetry curves unfold a typical CV of carbon-based structure. These regular, almost box-like CV curves without any remarkable redox peaks related to pseudo-faradaic reactions indicate that TEGN and MIGN both perform an ideal double layer capacitive behavior [20]. It is distinct that, in Fig. 3(c), TEGN showed larger CV area than MIGN, proving that the capacitance of TEGN electrode is higher than that of MIGN.

Fig. 4(a) illustrates the specific capacitance of the two samples at different current density. It can be observed that higher specific capacitance is obtained by TEGN at the same current density, which is in good accordance with CV results. In the case of TEGN, the maximum specific capacitance is up to 188 F/g at 0.1 A/g cur-

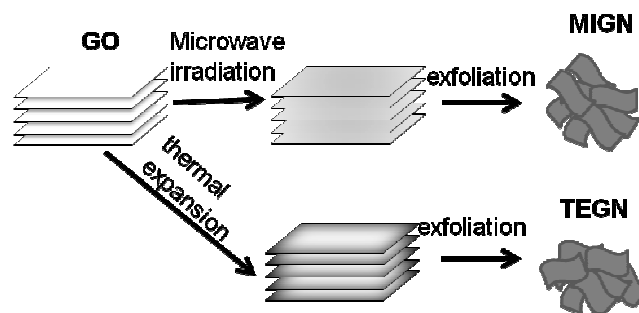


Figure 5. Representative scheme to show the mechanism of the two methods.

rent density while that of MIGN is 144 F/g at the same condition. It is commonly believed that the capacitance is closely correlated with the specific surface area [17]. The higher capacity of TEGN can be ascribed to the larger specific surface area (as shown in Table 1). Fig. 4(b) displays the capacitance versus cycle number for GNS samples at 0.1 A/g current density. The specific capacitance decreased much in the first cycle, which may be due to the oxygen-containing functional groups remaining on the surface of graphene nanosheets. Thereafter, the electrode reached a stable state. Besides, the capacitance retention of TEGN was 92% and that of MIGN was 97% over 500 charge–discharge cycles. This demonstrates that the as-obtained graphene-based supercapacitors perform good stability during long cycle charging/discharging.

#### 4. CONCLUSIONS

In summary, the influence of exfoliation methods on the microstructure and electrochemical property of GNS were investigated. The results showed that the electrochemical properties of GNS via thermal expansion are superior to those of GNS via microwave irradiation. In the process of exfoliation, thermal expansion produces more mesopores than MIGN. The BET surface area and pore volume of TEGN was much larger than that of MIGN. A maximum capacitance of 188 F/g for TEGN was observed at 0.1 A/g compared to 144 F/g for MIGN. The research would be attractive to prompt the application of graphene-based supercapacitors.

#### 5. ACKNOWLEDGEMENTS

We are grateful for the financial support from Project No.CDJZR10 13 88 01 & No.CDJXS10 13 11 58 of the Fundamental Research Funds for the Central Universities and for the Natural Science Foundation of China (No.51172293).

Table 1. The  $N_2$  absorption results of TEGN and MIGN.

Sample	BET Specific surface area( $m^2 g^{-1}$ )	Total pore volume( $cm^3 g^{-1}$ )	Average pore diameter(nm)
TEGN-1050	469	1.3	12.5
TEGN-800	325	1.2	15.0
TEGN-500	317	1.2	14.6
MIGN-800	354	1.1	12.3
MIGN-700	299	1.1	14.4
MIGN-500	264	1.0	15.5

## REFERENCES

- [1] M.A. Azam, A. Fujiwara, T. Shimoda, *Journal of New Materials for Electrochemical Systems*, 14, 173 (2011).
- [2] K.S. Novoselov, A.K. Geim, S.V. Morozov, et al., *Science*, 306, 666 (2004).
- [3] X. Wang, L. Zhi, K. Mullen, *Nano Letters*, 8, 323 (2007).
- [4] A.K. Geim, *Science*, 324, 1530 (2009).
- [5] T. Yumura, K. Kimura, H. Kobayashi, et al., *Physical Chemistry Chemical Physics*, 11, 8275 (2009).
- [6] V.C. Tung, M.J. Allen, Y. Yang, et al., *Nature Nanotechnology*, 4, 25 (2009).
- [7] M. Choucair, P. Thordarson, J.A. Stride, *Nature Nanotechnology*, 4, 30 (2009).
- [8] C.-a. Di, D. Wei, G. Yu, et al., *Advanced Materials*, 20, 3289 (2008).
- [9] A. Reina, X. Jia, J. Ho, et al., *Large Area, Nano Letters*, 9, 30 (2008).
- [10] K.S. Kim, Y. Zhao, H. Jang, et al., *Nature*, 457, 706 (2009).
- [11] C. Berger, Z.M. Song, X.B. Li, et al., *Science*, 312, 1191 (2006).
- [12] H. Huang, W. Chen, S. Chen, et al., *Acs Nano*, 2, 2513 (2008).
- [13] K.V. Emtsev, A. Bostwick, K. Horn, et al., *Nature Materials*, 8, 203 (2009).
- [14] H.C. Schniepp, J.L. Li, M.J. McAllister, et al., *Journal of Physical Chemistry B*, 110, 8535 (2006).
- [15] Y. Zhu, S. Murali, M.D. Stoller, et al., *Carbon*, 48, 2118 (2010).
- [16] D.C. Marcano, D.V. Kosynkin, J.M. Berlin, et al., *Acs Nano*, 4, 4806 (2010).
- [17] J. Chmiola, G. Yushin, R. Dash, et al., *Journal of Power Sources*, 158, 765 (2006).
- [18] J. Rouquerol, D. Avnir, C.W. Fairbridge, et al., *Pure and applied chemistry*, 66, 1739 (1994).
- [19] Q.-Y. Li, H.-Q. Wang, Q.-F. Dai, et al., *Solid State Ionics*, 179, 269 (2008).
- [20] M.D. Stoller, S. Park, Y. Zhu, et al., *Nano Letters*, 8, 3498 (2008).